Korean J Physiol Pharmacol
Vol 11: 183−188, October, 2007

Ca^{2+}-dependent Long-term Inactivation of Cardiac Na^+/Ca^{2+} Exchanger

Jee-Eun Lee, and Tong Mook Kang

Department of Physiology, SBRI, Sungkyunkwan University School of Medicine, Suwon 440-746, Korea

Using BHK cells with stable expression of cardiac Na^+/Ca^{2+} exchanger (BHK-NCX1), reverse mode (i.e. Ca^{2+} influx mode) of NCX1 current was recorded by whole-cell patch clamp. Repeated stimulation of reverse NCX1 produced a cytosolic Ca^{2+}-dependent long-term inactivation of the exchanger activity. The degrees of inactivation correlated with NCX1 densities of the cells and were attenuated by reduced Ca^{2+} influx via the reverse exchanger. The inactivation of NCX1 was attenuated by (i) inhibition of Ca^{2+} influx with reduced extracellular Ca^{2+}, (ii) treatment with NCX1 blocker (Ni^{2+}), and (iii) increase of cytoplasmic Ca^{2+} buffer (EGTA). In BHK-NCX1 cells transiently expressing TRPV1 channels, Ca^{2+} influx elicited by capsaicin produced a marked inactivation of NCX1. We suggest that cytoplasmic Ca^{2+} has a dual effect on NCX1 activities, and that allosteric Ca^{2+} activation of NCX1 can be opposed by the Ca^{2+}-dependent long-term inactivation in intact cells.

Key Words: Na^+/Ca^{2+} exchange, Calcium, Inactivation, TRPV1, BHK cell

INTRODUCTION

Cardiac Na^+/Ca^{2+} exchanger (NCX1) is the major Ca^{2+} extrusion mechanism during the cardiac action potential (Blaustein & Lederer, 1999). NCX1 is a bi-directional electrogenic Ca^{2+} transporter and contributes to electrical activity of the heart. The exchanger operates with multiple transport modes and has the major exchange ratio of $3Na^+$: $1Ca^{2+}$ (Reeves & Hale, 1984; Kang & Hilgemann, 2004). The direction of Ca^{2+} movement is determined by the electrochemical gradients for both Na^+ and Ca^{2+} across the membrane. The forward mode of NCX1 generates an inward current and removes Ca^{2+} out of the cells (i.e. Ca^{2+} efflux mode), while the reverse mode generates an outward current and brings Ca^{2+} into the cells (i.e. Ca^{2+} influx mode). Properties of NCX1 have been well characterized by excised giant patch clamp (Hilgemann, 1990), where the cytoplsasmic Na^+-dependent inactivation is ablated by the increased $[Ca^{2+}]_c$ and by membrane phosphatidylionositol-4,5-bisphosphate (PIP_2) (Hilgemann et al, 1992a; Hilgemann et al, 1992b; Hilgemann & Ball, 1996). These regulations are mediated via cytoplasmic loop domain of NCX1 and can be removed by enzymatic digestion of the loop with chymotrypsin (Hilgemann, 1990). Cytosolic Ca^{2+} modulates NCX1 activities by both direct allosteric Ca^{2+} activation (i.e. ablation of Na^+-inactivation) (Hilgemann et al, 1992b; Reeves & Condrescu, 2003) and multiple Ca^{2+} dependent cell signaling pathways (Iwamoto et al, 1998; Opuni & Reeves, 2000; Katanosaka et al, 2005; Zhang et al, 2006; Yaradanakul, 2007).

We have observed that, in Baby Hamster Kidney (BHK) cells stably expressing NCX1 (BHK-NCX1), Ca^{2+} influx by reverse exchanger undergoes inactivation in response to a repeated stimulation. This is rather unexpected, because it has been suggested that the allosteric Ca^{2+} activation of reverse exchanger persist for relatively long period after the termination of Ca^{2+} influx (Reeves & Condrescu, 2003). To address this issue, we recorded reverse exchanger current using whole-cell patch clamp from BHK-NCX1 cells, and presented evidence that the inactivation is generated by increased $[Ca^{2+}]_c$ and the degrees of inactivation correlate with the amount of Ca^{2+} influx.

METHODS

NCX1-expressing BHK cells

A stably NCX1-expressing BHK cells (BHK-NCX1) were kindly provided by Dr. K.D. Philipson (UCLA, USA). Cells were maintained and cultured as described elsewhere (Linck et al, 1998). Cells were detached with trypsin (0.25%) and used for whole-cell patch recordings. cDNA for rat TRPV1 was kindly provided by Dr. U. Oh (Seoul National University, Korea). The cDNA was subcloned in pIRES-EGFP (Clontech, USA) and expressed as a GFP fusion protein in BHK-NCX1 cells. The trasnsfection was performed in 35-mm dishes using *Lipofectamine 2000* (Invitrogen, USA) according to the manufacturer's manual, and the cells were incubated for 24~48 h.

Corresponding to: Tong Mook Kang, Department of Physiology, SBRI, Sungkyunkwan University School of Medicine, Suwon 440-746, Korea. (Tel) 82-31-299-6102, (Fax) 82-31-299-6129, (E-mail) tmkang@yurim.skku.ac.kr

ABBREVIATIONS: $[Ca^{2+}]c$, Cytosolic Ca^{2+} concentration; NMG, N-methyl-D-glucamine; EGTA, ethylene glycol-bis(2-amino-ethylether)-N,N,N',N',-tetra-acetic acid.

Whole-cell patch clamp

The cells were placed on an inverted microscope and superfused with bath solution through the chamber by gravity. The voltage clamp (Axopatch-1D, Axon Instruments, U.S.A.) was performed at room temperature (~24°C) with patch pipettes of 2~3 MΩ. Capacitance compensation was made and liquid junction potentials were corrected, and the currents were filtered at 5 kHz (-3 dB frequency) and sampled at 1 kHz. After finishing whole-cell current recording, membrane capacitance was measured with the capacitance compensation circuitry on the amplifier. Conventional whole-cell recording of reverse mode of NCX1 currents was performed with the pipette (cytoplasmic) solution containing (in mM): NaOH 50, NMG 70, CsOH 15, EGTA 10 (or 26), $CaCl_2$ 3.5, Hepes 50, $MgCl_2$ 0.7, Mg-ATP 2, and pH 7.2 adjusted with aspartic acid. '*Sliders v2.10*' (http://www.stanford.edu/~cpatton/downloads.htm) was used to calculate free [Ca^{2+}] of the pipette solution. When 10 mM EGTA was included in the pipette solution, calculated free [Ca^{2+}] and free [EGTA] were 100 nM and 6.3 mM, respectively. When EGTA was increased to 26 mM, calculated free [Ca^{2+}] and free [EGTA] were 30 nM and 21.9 mM, respectively. Extracellular bath solution contained (in mM): NaOH 30, NMG 120, EGTA 0.5, $CaCl_2$ 3.5 (or 0 for Ca^{2+}-free), Hepes 15, $MgCl_2$ 2, glucose 10, and pH 7.4 adjusted with aspartic acid. At a holding potential of 0 mV, an alternative perfusion of Ca^{2+}-free bath solution turned off NCX1, and a standard 3 mM Ca^{2+}-containing bath solution (i.e. Ca^{2+} pulse) turned on NCX1.

Chemicals and statistics

All chemicals were purchased from Sigma. Values given in the text are mean±S.E.M. with *n*, the sample size. Significant differences were detected using Student's *t* test (*: $p<0.05$, **: $p<0.01$).

RESULTS

Long-term inactivation of reverse NCX1 current

Reverse mode of outward NCX1 currents was activated multiple times, at every ~50 s intervals, by applying 3 mM Ca^{2+} pulses. The peak current recorded during the first Ca^{2+} pulse (denoted as '1st NCX' in Fig. 1A) decayed by >70% over ~30 sec (Fig. 1A). Neither amplitudes nor decay of the 1st NCX1 required internal Ca^{2+} release, because inclusion of an endoplasmic reticulum Ca^{2+}-ATPase inhibitors such as cyclopiazonic acid (20 μM) or thapsigargin (1 μM) had no effect on the current (data not shown). NCX1 currents activated by the second Ca^{2+} pulse (denoted as '2nd NCX' in Fig. 1A) were ~20% of the 1st NCX1. After activating NCX1 multiple times, the exchanger currents did not recover to the amplitudes of the 1st NCX1, and therefore, we named it 'long-term inactivation' of reverse NCX1. When Ca^{2+} pulses were applied >15 min after achieving whole-cell configuration, the same inactivation was recorded, suggesting that neither insufficient dialysis of the pipette solution nor loss of diffusible factor(s) through the patch pipette mediates the inactivation (data not shown). Although data are not presented here, we emphasize that (i) the increase of $[Ca^{2+}]_c$ by repeated stimulation of the reverse exchanger undergoes long-term inactivation in fura-2 loaded BHK-NCX1 cells, and (ii) the reverse exchanger currents recorded from excised inside-out giant patches are not inactivated significantly by a repeated stimulation.

Relationship between NCX1 densities and degrees of inactivation

As presented in Fig. 1B, ~20% of BHK-NCX1 cells showed smaller exchanger current and weaker inactivation. To define the relationship between the current amplitudes and degrees of inactivation, amplitudes of the 2nd NCX1 were normalized to the 1st NCX1 (denoted as '% of the 1st NCX') and then plotted against exchanger densities of the 1st NCX1 (pA/pF). We divided cells into two groups; i.e., cells with lower NCX1 densities (<10 pA/pF) and ones with higher densities (>10 pA/pF). Cell capacitances measured were not different between the groups (12.6±0.7 pF for lower density vs. 13.2±0.7 pF for higher density), suggesting that they have different expression levels of functional surface NCX1. As shown in Fig. 1C, cells with lower densities (8.6±0.3 pA/pF, n=17) were weakly inactivated (55.7±6.0%), while ones with higher densities (17.8±1.0 pA/pF, n=36) were strongly inactivated (16.5±1.5%, $p<0.01$). The cells with higher densities were markedly inactivated by the 2nd Ca^{2+} pulse. On the contrary, the cells with lower densities showed a progressive inactivation in response to repeated stimulation (Fig. 1D). The data suggest that the expression level of NCX1 determines the amount of Ca^{2+} influx via reverse exchanger, thereby setting the degrees of inactivation.

Relationship between the amounts of Ca^{2+} influx and degrees of inactivation

To better define the correlation between the amounts of Ca^{2+} influx and the degrees of inactivation, NCX1 amplitudes were reduced by decreasing extracellular [Ca^{2+}] or by treating cells with NCX1 blocker, nickel (Ni^{2+}) (Fig. 2). As shown in Fig. 2A and B, NCX1 currents by 1.5 or 3 mM Ca^{2+} pulses were inactivated to the same extent (2nd NCX1; 15.2±7.0% for 1.5 mM Ca^{2+} and 16.2±2.5% for 3 mM Ca^{2+}, n=5~7). Meanwhile, 0.1 mM Ca^{2+} pulses significantly attenuated the normalized inactivation (2nd NCX1=76.1±5.4%, n=5, $p<0.01$ compared to 3 mM Ca^{2+}). As expected, this was mainly due to decreased Ca^{2+} influx with reduced extracellular Ca^{2+}.

NCX1 currents were dose-dependently reduced by Ni^{2+} and the normalized inactivation was reduced as Ni^{2+} increased (Fig. 2C and D). In the presence of Ni^{2+} (2.5, 5, or 7 mM), 3 mM Ca^{2+} pulses were applied five times and Ni^{2+} was then removed, and the repeated Ca^{2+} pulses were followed. A lower concentration of Ni^{2+} (2.5 mM) induced inactivation of NCX1 by >90% during five repeated pulses (5th NCX1=8.6±0.6%, n=4). When the Ni^{2+} removed, NCX1 currents were hardly recovered from the inactivation (6th NCX1=12.1±2.1%, n=4). On the contrary, a higher concentration of Ni^{2+} (7 mM) strongly reduced the exchanger current, and NCX1 was weakly inactivated by 43% during first 5 repeated pulses (5th NCX1=57.1±2.3%, n=5). These values are comparable to that with 0.1 mM Ca^{2+} pulses, shown in Fig. 2B. After removing the Ni^{2+}, NCX1 increased to 302.8±72.7% (6th NCX1, open arrows). Then, the 7th NCX1 (closed arrows) was markedly inactivated to 56.6±16.1%,

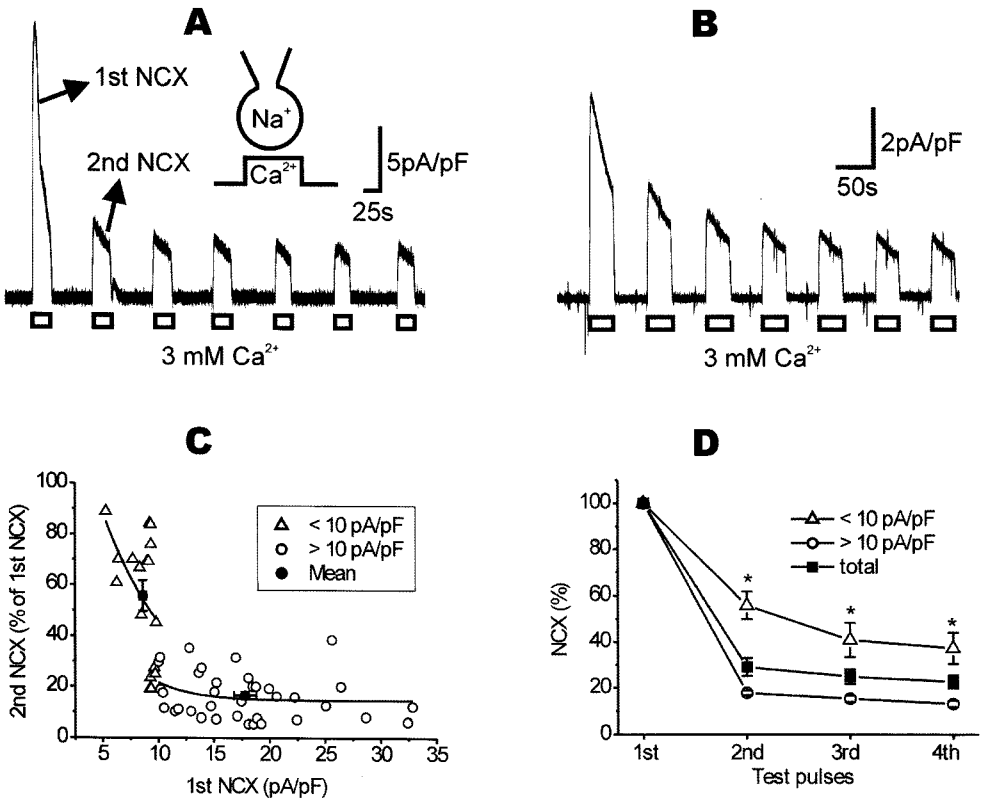

Fig. 1. Relationship between NCX1 densities and degrees of NCX1 inactivation. A stronger inactivation of reverse mode of NCX1 current was recorded from the cells with higher NCX1 densities (A), while the cells with lower NCX1 densities showed a weaker inactivation (B). (C) NCX1 currents recorded during the 2nd Ca^{2+} pulse were normalized to the 1st NCX1 current and expressed on y-axis as '% of 1st NCX' and plotted against NCX1 densities ('1st NCX' expressed in pA/pF). For comparison, degrees of inactivation of the cells with <10 pA/pF (△) and ones with >10 pA/pF (○) are separately illustrated. Mean values of inactivation and NCX1 densities from each group (■) are described in text. To clarify the relation between NCX1 densities and % inactivation, data points from each group were fitted with a single exponential function. (D) The time courses of inactivation in response to repeated Ca^{2+} pulses at every ~50 s intervals are illustrated. The cells with higher NCX1 densities (△) and ones with lower densities (○) are compared with mean values of total data (■). *: $p<0.05$ compare to total.

due to Ca^{2+} entered during the 6th pulse (Fig. 2C and D). Inactivation of the 7th NCX1 was ~19% of the 6th NCX1 (i.e. 302 vs. 57%), and it's value is comparable to the 2nd NCX1 in the absence of Ni^{2+} (~16%, Fig. 1D) or with 2.5 mM Ni^{2+} (10.0±2.6%, Fig. 2D).

Increased cytoplasmic Ca^{2+} buffer attenuates the inactivation of NCX1

Reduction of inactivation is expected by increasing cytoplasmic Ca^{2+} buffer. Therefore, in order to prove it, NCX1 was recorded by pipette solution with a higher Ca^{2+} buffer (26 mM EGTA+3.5 mM Ca^{2+} instead of 10 mM EGTA+3.5 mM Ca^{2+}). As shown in Fig. 3 ('high-EGTA'), the 1st NCX1 current increased by ~2 folds with higher cytoplasmic EGTA (15.5±1.9 pA/pF for control *vs.* 30.3±5.3 pA/pF for high-EGTA, $p<0.05$) (Fig. 3B). This is due to increased Ca^{2+} gradient across the membrane, since $[Ca^{2+}]_c$ was decreased from 100 to 30 nM by increasing concentration of EGTA. With higher concentration of EGTA, degrees of inactivation were reduced by ~50% of the control (2nd NCX1; 18.1±3.1% of the 1st NCX1 for control vs. 35.7±4.7% for high-EGTA, $p<0.05$) (Fig. 3B). However, it was still much stronger (~64% inactivation) than the inactivation occurred with 0.1 mM extracellular Ca^{2+} or with 7 mM Ni^{2+} (~25% inactivation; Fig. 2).

Ca^{2+} influx through TRPV1 channels inactivates NCX1

Next, we examined whether Ca^{2+} influx via pathways other than the reverse exchanger can inactivate NCX1. Thus, TRPV1 channels were selected as an alternative Ca^{2+} influx pathway, since the channels are highly Ca^{2+}-selective and selectively activated with an agonist, capsaicin. As shown in Fig. 4, BHK-NCX1 cells were transiently transfected with TRPV1 channels and were stimulated with capsaicin to elicit Ca^{2+} entry through the channels. Ca^{2+} influx via the reverse exchanger was diminished by 10 mM Ni^{2+}, and 3 mM Ca^{2+} pulse was then applied along with 1 μM capsaicin. In control cells transfected with GFP alone, the Ca^{2+} pulse together with capsaicin elicited a smaller out-

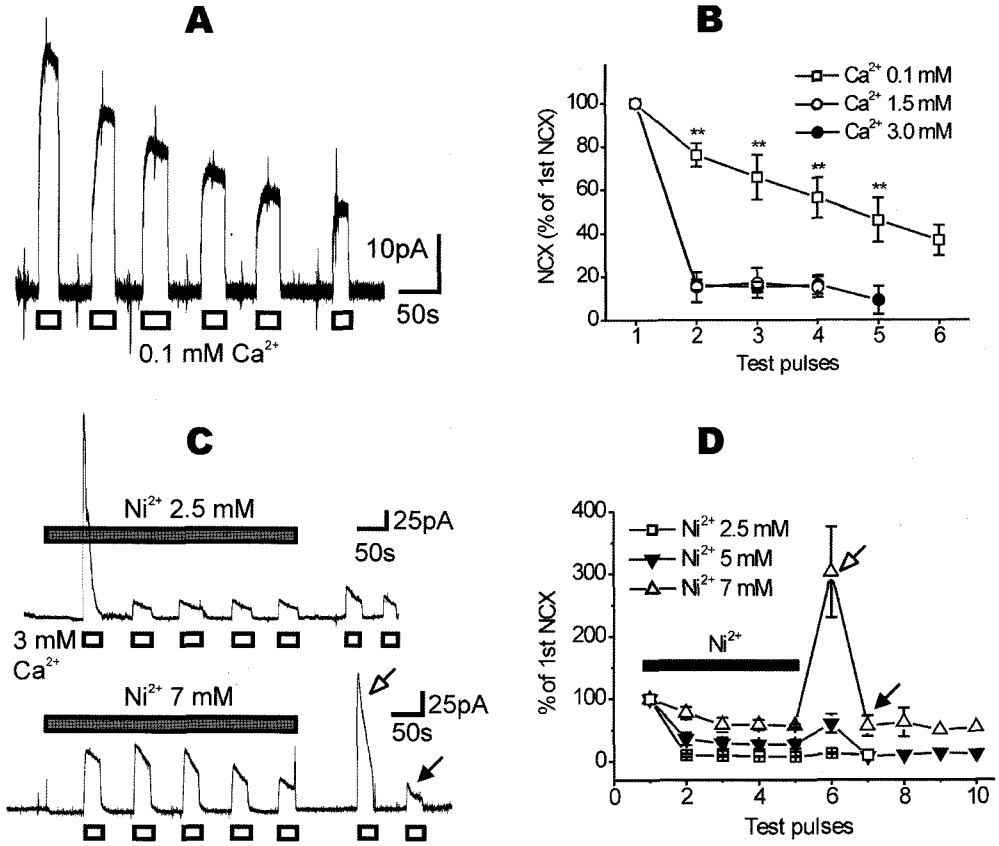

Fig. 2. Relationship between the amounts of Ca^{2+} influx and degrees of inactivation. (A) Current traces showing a weaker inactivation in response to 0.1 mM Ca^{2+} pulses. (B) Inactivation time courses with 0.1, 1.5 and 3 mM Ca^{2+} pulses are summarized. (C and D) In presence of 2.5 mM Ni^{2+}, NCX1 inactivated by >90% during the first 5 repeated Ca^{2+} pulses, and it remained inactivated after removing Ni^{2+}. In the presence of 5 or 7 mM Ni^{2+}, NCX1 was weakly inactivated during the first 5 repeated pulses. After removing Ni^{2+}, NCX1 was recovered from Ni^{2+} inhibition (open arrows). Then, the 7^{th} NCX1 currents (closed arrows) became inactivated due to Ca^{2+} entered during the 6^{th} pulse.

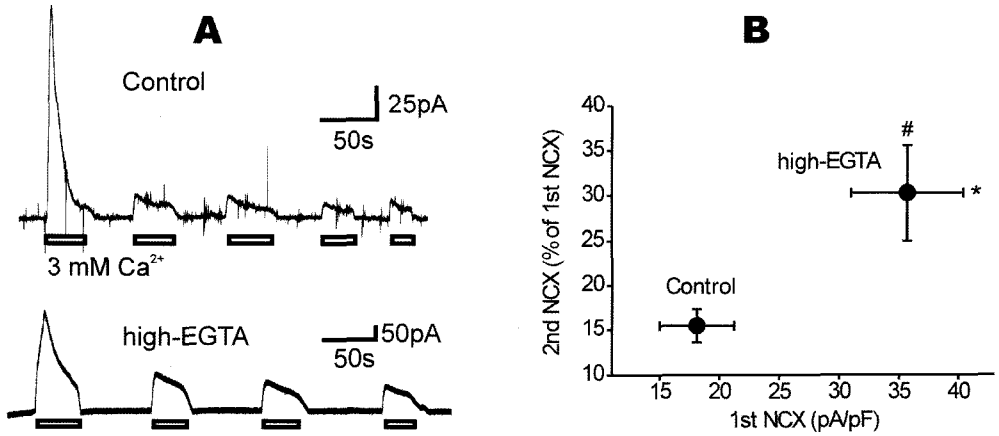

Fig. 3. Effect of increased cytoplasmic Ca^{2+} buffer on the NCX1 inactivation. In the recording pipette, 26 mM EGTA with 3.5 mM Ca^{2+} (high-EGTA) was included. Control cells were recorded with 10 mM EGTA along with 3.5 mM Ca^{2+}. (A) Representative recordings with standard 3 mM Ca^{2+} pulses are illustrated. (B) Degrees of inactivation during the 2^{nd} Ca^{2+} pulses are expressed as '% of 1^{st} NCX' on y-axis, and plotted against the current densities of the 1^{st} NCX1 current. The marks above the error bars represent statistical significance ($p < 0.05$) compared to the control responses. Detailed values are described in the text.

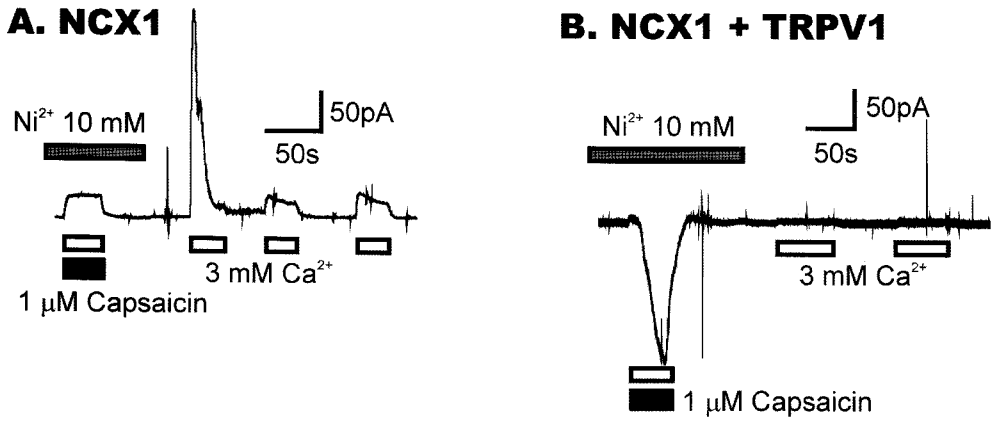

Fig. 4. Ca^{2+} influx through TRPV1 Ca^{2+} channels inactivates NCX1. BHK-NCX1 cells were transiently expressed with rat TRPV1 channels and stimulated with capsaicin to elicit Ca^{2+} entry through the channels. At the beginning, Ca^{2+} influx via reverse exchanger was limited by 10 mM Ni^{2+}. (A) Capsaicin had no effect on the Ca^{2+}-dependent inactivation in control BHK-NCX1 cells. (B) 3 mM Ca^{2+} pulse applied together with 1 μM capsaicin produced an inward current in TRPV1-expressed cells, and produced strong inactivation of NCX1.

ward exchanger current. When Ni^{2+} and capsaicin were removed, exchanger current was restored during the 2nd pulse, and then the 3rd NCX1 showed a strong inactivation (Fig. 4A). On the other hand, TRPV1-expressed BHK-NCX1 cells produced capsaicin-induced inward Ca^{2+} current. By removing Ni^{2+}, NCX1 was not recovered and remained inactivated during repeated Ca^{2+} pulses (Fig. 4B). The data clearly suggest that the Ca^{2+} entered via TRPV1 channels generates strong inactivation of NCX1. Under our experimental conditions, the contribution of entered Na^+ through TRPV1 channels might be excluded because the cytoplasmic $[Na^+]$ was clamped at 50 mM using a pipette solution.

DISCUSSION

In this study, we have demonstrated that the increase of cytoplasmic Ca^{2+} concentration produces a long-term inactivation of NCX1 activities. Although we can not offer any underlying mechanism of the Ca^{2+}-dependent inactivation at this time, it is striking to note that higher increase of $[Ca^{2+}]_c$ produces stronger inactivation. Further studies are required to fully understand underlying mechanism of the Ca^{2+}-dependent inactivation of NCX1 and its physiological and pathological implications in intact cells.

It is well known that $[Ca^{2+}]_c$ rises both during and after the periods of hypoxia or ischemia. It has been demonstrated that $[Ca^{2+}]_c$ increase during reperfusion or reoxygenation is mainly caused by Ca^{2+} entry through reverse mode of NCX1 (Haigney et al, 1992). If the initial rise in $[Ca^{2+}]_c$ during the period of hypoxia inactivates NCX1's activities, it can attenuate the deteriorating Ca^{2+} entry through reverse exchanger during the periods of reoxygenation or reperfusion. Expression of NCX has been demonstrated in TRPV1-expressing nociceptive rat dorsal root ganglion (DRG) neurons (Verdru et al, 1997). In the present study, we showed that Ca^{2+} entry via TRPV1 channels strongly inactivates NCX1 (Fig. 4). In native DRG neurons, therefore, rise of $[Ca^{2+}]_c$ by strong activation of TRPV1 channels by noxious stimuli (i.e. heat, acid, inflammatory mediators, capsaicin) can inactivate the exchanger's activities. When Ca^{2+} extrusion by the exchangers is inhibited, neurons can easily be excited by noxious stimuli, and thereby, sensitizes to nociceptive responses.

Similar to our present results, an inactivation of reverse exchanger with repeated stimulation has been reported in fura-2 loaded CHO-NCX1 cells (Opuni & Reeves, 2000). Since the inhibition of mitochondrial Ca^{2+} uptake prevented the inactivation, they suggested that an inhibitory signal generated during mitochondrial Ca^{2+} sequestration plays a role. Therefore, the role of mitochondria played in NCX1 inactivation of BHK remains to be elucidated. It has been suggested that increasing surface PIP_2 rapidly activates endocytosis of NCX1 protein and produces long-term reduction of the whole-cell current in several minutes (Condrescu & Reeves, 2006; Yaradanakul et al, 2007; Shen et al, 2007). They also suggested that PLC activity, higher $[Ca^{2+}]_c$, and integrity of actin cytoskeletons can influence the trafficking of NCX1. The PIP_2-dependent trafficking rate is much higher than the 'functional half-life' of NCX1 proteins into or out of internal compartments (Egger et al, 2005), possibly suggesting that cytosolic Ca^{2+}-activated PIP_2 metabolism is important for the generation of inactivation. To address this issue, trafficking of NCX1 protein during Ca^{2+}-dependent inactivation period should be studied.

In summary, we suggest that cytoplasmic Ca^{2+} has a dual effect on NCX1 activities. It is highly likely that NCX1 is under the opposing influence of cytosolic Ca^{2+}, and that direct allosteric Ca^{2+} activation of NCX1 can be opposed by Ca^{2+}-induced long-term inactivation in intact cells.

ACKNOWLEDGEMENT

We thank Kenneth D. Philipson (UCLA, USA) for BHK-NCX1 cell lines, Uhtaek Oh (Seoul National University, Korea) for TRPV1 cDNA, and Donald W. Hilgemann (UT Southwestern, USA) for an advice. This work was supported by the Korea Research Foundation Grant (KRF-2004-041-E00012).

REFERENCES

Blaustein MP, Lederer WJ. Sodium/calcium exchange: its physiological implications. *Physiol Rev* 79:763–854, 1999

Condrescu M, Reeves JP. Actin-dependent regulation of the cardiac Na^+/Ca^{2+} exchanger. *Am J Physiol Cell Physiol* 290: C691–701, 2006

Egger M, Porzig H, Niggli E, Schwaller B. Rapid turnover of the "functional" Na^+-Ca^{2+} exchanger in cardiac myocytes revealed by an antisense oligodeoxynucleotide approach. *Cell Calcium* 37: 233–243, 2005

Haigney MC, Miyata H, Lakatta EG, Stern MD, Silverman HS. Dependence of hypoxic cellular calcium loading on Na^+-Ca^{2+} exchange. *Circ Res* 71: 547–557, 1992

Hilgemann DW, Ball R. Regulation of cardiac Na^+, Ca^{2+} exchange and K_{ATP} potassium channels by PIP_2. *Science* 273: 956–959, 1996

Hilgemann DW, Collins A, Matsuoka S. Steady-state and dynamic properties of cardiac sodium-calcium exchange. Secondary modulation by cytoplasmic calcium and ATP. *J Gen Physiol* 100: 933–961, 1992b

Hilgemann DW, Matsuoka S, Nagel GA, Collins A. Steady-state and dynamic properties of cardiac sodium-calcium exchange. Sodium-dependent inactivation. *J Gen Physiol* 100: 905–932, 1992a

Hilgemann DW. Regulation and deregulation of cardiac Na^+-Ca^{2+} exchange in giant excised sarcolemmal membrane patches. *Nature* 344: 242–245, 1990

Iwamoto T, Pan Y, Nakamura TY, Wakabayashi S, Shigekawa M. Protein kinase C-dependent regulation of Na^+/Ca^{2+} exchanger isoforms NCX1 and NCX3 does not require their direct phosphorylation. *Biochemistry* 37: 17230–17238, 1998

Kang TM, Hilgemann DW. Multiple transport modes of the cardiac Na^+/Ca^{2+} exchanger. *Nature* 427: 544–548, 2004

Katanosaka Y, Iwata Y, Kobayashi Y, Shibasaki F, Wakabayashi S, Shigekawa M. Calcineurin inhibits Na^+/Ca^{2+} exchange in phenylephrine-treated hypertrophic cardiomyocytes. *J Biol Chem* 280: 5764–5772, 2005

Linck B, Qiu Z, He Z, Tong Q, Hilgemann DW, Philipson KD. Functional comparison of the three isoforms of the Na^+/Ca^{2+} exchanger (NCX1, NCX2, NCX3). *Am J Physiol* 274: C415–423, 1998

Opuni K, Reeves JP. Feedback inhibition of sodium/calcium exchange by mitochondrial calcium accumulation. *J Biol Chem* 275: 21549–21554, 2000

Reeves JP, Condrescu M. Allosteric activation of sodium-calcium exchange activity by calcium: persistence at low calcium concentrations. *J Gen Physiol* 122: 621–639, 2003

Reeves JP, Hale CC. The stoichiometry of the cardiac sodium-calcium exchange system. *J Biol Chem* 259: 7733–7739, 1984

Shen C, Lin MJ, Yaradanakul A, Lariccia V, Hill JA, Hilgemann DW. Dual control of cardiac Na^+/Ca^{2+} exchange by PIP_2: analysis of the surface membrane fraction by extracellular cysteine PEGylation. *J Physiol* 582: 1011–1026, 2007

Verdru P, De Greef C, Mertens L, Carmeliet E, Callewaert G. Na^+-Ca^{2+} exchange in rat dorsal root ganglion neurons. *J Neurophysiol* 77:484–90, 1997

Yaradanakul A, Feng S, Shen C, Lariccia V, Lin MJ, Yang J, Kang TM, Dong P, Yin HL, Albanesi JP, Hilgemann DW. Dual control of cardiac Na^+/Ca^{2+} exchange by PIP_2: electrophysiological analysis of direct and indirect mechanisms. *J Physiol* 582: 991–1010, 2007

Zhang XQ, Ahlers BA, Tucker AL, Song J, Wang J, Moorman JR, Mounsey JP, Carl LL, Rothblum LI, Cheung JY. Phospholemman inhibition of the cardiac Na^+/Ca^{2+} exchanger. Role of phosphorylation. *J Biol Chem* 281: 7784–7792, 2006